

Self-Assembly of an Azido-Bridged $[\text{Ni}^{\text{II}}_6]$ Cluster Featuring Four Fused Defective CubanesDebashree Mandal,[†] Valerio Bertolasi,[‡] Jordi Ribas-Ariño,[§] Guillem Aromí,^{*||} and Debashis Ray^{*†}

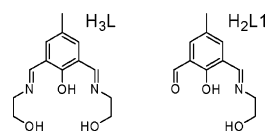
Department of Chemistry, Indian Institute of Technology, Kharagpur 721 302, India, Dipartimento di Chimica e Centro di Strutturistica Diffraattometrica, Università di Ferrara, via L. Borsari 46, 44100 Ferrara, Italy, Lehrstuhl für Theoretische Chemie, Ruhr-Universität-Bochum, Universitätstrasse 150, D-44801 Bochum, Germany, and Department de Química Inorgànica, Facultat de Química, Universitat de Barcelona, Diagonal 647, 08028 Barcelona, Spain

Received January 30, 2008

The cluster $[\text{Ni}_6(\text{H}_2\text{L})_2(\text{HL}1)_2(\text{N}_3)_8] \cdot 2\text{C}_2\text{H}_5\text{OH} \cdot 2\text{H}_2\text{O} [1 \cdot 2\text{C}_2\text{H}_5\text{OH} \cdot 2\text{H}_2\text{O}]$, featuring four fused defective cubanes, has been obtained via azido-bridge-driven dimerization of two phenolate-centered trinuclear Ni_3 fragments.

High-nuclearity transition-metal spin clusters are of prime importance in the area of molecular magnetism.^{1,2} For example, single-molecule magnets were discovered with a dodecanuclear manganese aggregate,³ and since then, many more examples have been prepared.⁴ This category of compounds is typically prepared via self-assembly processes by combining metal ions with the appropriate bridging and/or blocking ligands, where the final outcome is never predicted beforehand.⁵ A structural feature commonly encountered within this chemistry is that of “fused defective cubanes”.^{6–12} In these, the vertices are composed of either the metals or ligand donor atoms (μ - and μ_3 -N or -O). The

Scheme 1



azide group is a very suitable bridging ligand in the construction of this motif, and its relevance in cluster coordination chemistry has recently increased.¹³ Nickel clusters involving azide ligands as bridges are, however, still scarce. The existing azide-based nickel clusters comprising fused cubanes feature the nuclearities $[\text{Ni}_4]$,^{14,15} $[\text{Ni}_8]$,¹⁶ and $[\text{Ni}_{10}]$.¹⁷ A remarkable absence in this list of compounds is that of an $[\text{Ni}_6]$ species. In this context, we have explored the reactivity of polynucleating Schiff base ligand H_3L (Scheme 1, left) with the $\text{Ni}^{\text{II}}/\text{N}_3^-$ system. The use of this ligand in polynuclear transition-metal chemistry is relatively new, although some remarkable results have been reported, consisting of a $[\text{Cu}^{\text{II}}_{18}]$ ¹⁸ cluster and a heterometallic $[\text{Mn}_6\text{Cu}_{10}]$ species.¹⁹ The aggregating ability of H_3L , together with the bridging properties of azide, has now been exploited here with the preparation of the novel hexanuclear complex $[\text{Ni}_6(\text{H}_2\text{L})_2(\text{HL}1)_2(\text{N}_3)_8]$ (**1**), revealing partial hydrolysis of the original Schiff base ligand.

* To whom correspondence should be addressed. E-mail: guillem.aromi@qi.ub.es (G.A.), dray@chem.iitkgp.ernet.in (D.R.).

[†] Indian Institute of Technology.

[‡] Università di Ferrara.

[§] Ruhr-Universität-Bochum.

^{||} Universitat de Barcelona.

- (1) Christou, G.; Gatteschi, D.; Hendrickson, D. N.; Sessoli, R. *MRS Bull.* **2000**, 25, 66–71.
- (2) Gatteschi, D. *Adv. Mater.* **1994**, 6, 635–645.
- (3) Sessoli, R.; Tsai, H. L.; Schake, A. R.; Wang, S. Y.; Vincent, J. B.; Foltling, K.; Gatteschi, D.; Christou, G.; Hendrickson, D. N. *J. Am. Chem. Soc.* **1993**, 115, 1804–1816.
- (4) Aromí, G.; Brechin, E. K. *Struct. Bonding (Berlin)* **2006**, 122, 1–67.
- (5) Winpenny, R. E. P. *J. Chem. Soc., Dalton Trans.* **2002**, 1–10.
- (6) Rajaraman, G.; Murugesu, M.; Sanudo, E. C.; Soler, M.; Wernsdorfer, W.; Helliwell, M.; Muryn, C.; Raftery, J.; Teat, S. J.; Christou, G.; Brechin, E. K. *J. Am. Chem. Soc.* **2004**, 126, 15445–15457.
- (7) Glaser, T.; Lugger, T.; Hoffmann, R. D. *Eur. J. Inorg. Chem.* **2004**, 2356–2362.
- (8) Pashchenko, V.; Brendel, B.; Wolf, B.; Lang, M.; Lyssenko, K.; Shchegolikina, O.; Molodtsova, Y.; Zherlitsyna, L.; Auner, N.; Schutz, F.; Kollar, M.; Kopietz, P.; Harrison, N. *Eur. J. Inorg. Chem.* **2005**, 4617–4625.
- (9) Gigant, K.; Rammal, A.; Henry, M. *J. Am. Chem. Soc.* **2001**, 123, 11632–11637.
- (10) Abbati, G. L.; Cornia, A.; Fabretti, A. C.; Caneschi, A.; Gatteschi, D. *Inorg. Chem.* **1998**, 37, 3759–3766.

- (11) Goodwin, J. C.; Sessoli, R.; Gatteschi, D.; Wernsdorfer, W.; Powell, A. K.; Heath, S. L. *J. Chem. Soc., Dalton Trans.* **2000**, 1835–1840.
- (12) Aromí, G.; Batsanov, A. S.; Christian, P.; Helliwell, M.; Parkin, A.; Parsons, S.; Smith, A. A.; Timco, G. A.; Winpenny, R. E. P. *Chem.—Eur. J.* **2003**, 9, 5142–5161.
- (13) Escuer, A.; Aromí, G. *Eur. J. Inorg. Chem.* **2006**, 4721–4736.
- (14) Karmakar, T. K.; Chandra, S. K.; Ribas, J.; Mostafa, G.; Lu, T. H.; Ghosh, B. K. *Chem. Commun.* **2002**, 2364–2365.
- (15) Serna, Z. E.; Lezama, L.; Urtiaga, M. K.; Arriortua, M. I.; Barandika, M. G.; Cortes, R.; Rojo, T. *Angew. Chem., Int. Ed.* **2000**, 39, 344–347.
- (16) Bell, A.; Aromí, G.; Teat, S. J.; Wernsdorfer, W.; Winpenny, R. E. P. *Chem. Commun.* **2005**, 2808–2810.
- (17) Aromí, G.; Parsons, S.; Wernsdorfer, W.; Brechin, E. K.; McInnes, E. J. L. *Chem. Commun.* **2005**, 5038–5040.
- (18) Shiga, T.; Maruyama, K.; Han, L. Q.; Oshio, H. *Chem. Lett.* **2005**, 34, 1648–1649.
- (19) Yamashita, S.; Shiga, T.; Kurashina, M.; Nihei, M.; Nojiri, H.; Sawa, H.; Kakiuchi, T.; Oshio, H. *Inorg. Chem.* **2007**, 46, 3810–3812.

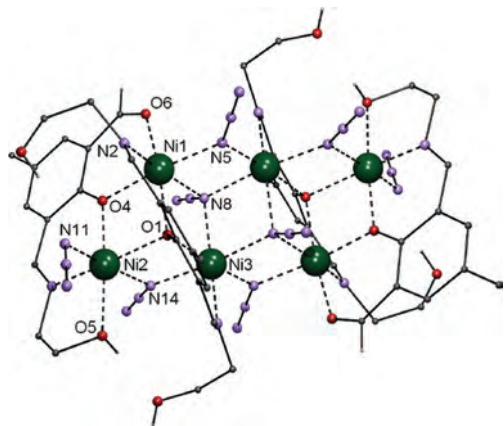
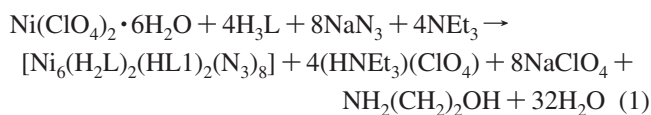


Figure 1. PovRay representation of **1**. Core atoms of the asymmetric unit are labeled. Gray balls are carbon atoms. Only hydrogen atoms from aldehyde or alcohol functions are shown (smallest balls). The whole molecule is generated through the symmetry operation $[1-x, 1-y, -z]$.

Complex **1**·2C₂H₅OH·2H₂O was obtained as a precipitate in 86% yield from EtOH, as proposed in eq 1.



The Schiff base had been prepared (Scheme S1 in the Supporting Information) as previously published.²⁰ The formula of **1** contains two HL¹⁻ ligands (Scheme 1, right), which originate from the hydrolysis of one of the arms of H₃L, as assisted presumably by the metals. Interestingly, such a hydrolysis product has not been observed as part of previous clusters obtained with H₃L.^{18,19}

The crystallographic asymmetric unit is built up by a trinuclear Ni^{II} fragment and two solvent-disordered molecules of water and ethanol. Complex **1**²¹ (Figures 1 and S1 and S2 in the Supporting Information) is a Ni^{II} centrosymmetric cluster in the form of four fused defective cubes with a [Ni₆O₄N₆] core (Figures S3 and S4 in the Supporting Information), where the bridging is ensured by six end-on (EO) azide ligands (four μ^- and three μ_3 -N₃⁻) and four phenolate moieties (two μ , from H₂L⁻, and two μ_3 , from HL¹⁻). The remaining coordination sites of the octahedral Ni^{II} ions are completed by peripheral imine groups (from H₂L⁻ and HL¹⁻), aldehyde functions, or alcohol residues (the latter two from HL¹⁻). Interestingly, both alcohol arms of the ligand H₂L⁻ remain uncoordinated and engaged in hydrogen-bonding interactions. Inspection of Figure 1 suggests indeed that the formation of **1** occurs through dimerization of two such trinuclear fragments (Scheme S2 in the Supporting Information). While the N₃⁻ bridging modes present in this complex are quite common, the μ_3 -phenoxide feature observed in **1** (Figures S5–S7 in the Supporting

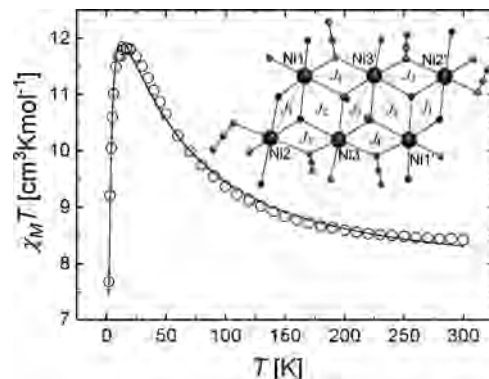


Figure 2. Plot of $\chi_M T$ vs T per mole of **1**. The solid line is the best fit to the experimental data (see the text). The inset is a scheme of the core of **1**, indicating the labels used for the spin Hamiltonian considered for the fit.

Information) is rather exceptional, although not unknown.^{22–24} The unprecedented ladder-type Ni₆ arrangement (Figure S8 in the Supporting Information) of complex **1** results from the peculiar preferences of H₂L⁻ and HL¹⁻ in front of the Ni^{II}/N₃⁻ system, as opposed to other well-established structures observed for Ni^{II} clusters with similar sets of ligands, such as cubanes,²⁵ tetranuclear defective dicubanes,¹⁵ or star-shaped complexes²⁶ (Scheme S3 in the Supporting Information).

The magnetic properties of **1** were investigated through variable-temperature susceptibility measurements. The resulting $\chi_M T$ vs T plot is given in Figure 2. In this plot, the value of $\chi_M T$ at 300 K is 8.4 cm³ K mol⁻¹ (slightly above that expected for six uncoupled octahedral Ni^{II} centers with $g = 2.2$; 7.3 cm³ K mol⁻¹) and increases with cooling to reach a maximum of 11.82 cm³ K mol⁻¹ at 17 K. With further cooling, the product of $\chi_M T$ decreases down to 7.7 cm³ K mol⁻¹ at 2 K. This curve indicates that the exchange within **1** is dominated by ferromagnetic interactions; however, it remains ambiguous about the ground state. The maximum could be due to the existence of some intramolecular antiferromagnetic interactions (which would cause the ground state to be lower than $S_T = 6$), to the presence of zero-field splitting (ZFS), to antiferromagnetic exchange between clusters, or to a combination of any of these three factors. Because the three are expected to be strongly correlated, it is necessary to have some previous information before attempting to fit the experimental data. Density functional theory (DFT) calculations were thus performed in order to get an estimate of the coupling constants within the cluster (Figure S9 in the Supporting Information). These were conducted with the *Gaussian 03* program,²⁷ using the B3LYP functional,²⁸ and an Ahlrichs TZV basis set²⁹ for the Ni ions and an Ahlrichs DZV basis set³⁰ for the rest were obtained

(20) Gagne, R. R.; Spiro, C. L.; Smith, T. J.; Hamann, C. A.; Thies, W. R.; Shiemke, A. K. *J. Am. Chem. Soc.* **1981**, *103*, 4073–4081.

(21) Crystallographic data were collected at 295 K on a Nonius Kappa CCD diffractometer with Mo K α radiation ($\lambda = 0.71073$ Å). Crystal data for compound **1**: C₅₂H₇₄N₃₀O₁₆Ni₆ ($M_w = 1727.67$), monoclinic, space group $P2_1/c$, $a = 14.9272(2)$ Å, $b = 13.4717(2)$ Å, $c = 17.3886(3)$ Å, $\beta = 93.5839(8)^\circ$, $V = 3489.92(9)$ Å³, $Z = 2$, $D_c = 1.644$ g cm⁻³, $\mu = 1.672$ mm⁻¹, $R1 = 0.0462$, $wR2 = 0.1227$. All non-hydrogen atoms were refined anisotropically. CCDC-616808.

(22) Aromí, G.; Batsanov, A. S.; Christian, P.; Helliwell, M.; Roubeau, O.; Timco, G. A.; Winpenny, R. E. P. *Dalton Trans.* **2003**, 4466–4471.

(23) Cromie, S.; Launay, F.; McKee, V. *Chem. Commun.* **2001**, 1918–1919.

(24) Mukherjee, S.; Weyhermüller, T.; Bothe, E.; Wieghardt, K.; Chaudhuri, P. *Eur. J. Inorg. Chem.* **2003**, 863–875.

(25) Halcrow, M. A.; Huffman, J. C.; Christou, G. *Angew. Chem., Int. Ed.* **1995**, *34*, 889–891.

(26) Ribas, J.; Monfort, M.; Costa, R.; Solans, X. *Inorg. Chem.* **1993**, *32*, 695–699.

(27) *Gaussian 03*, revision C.02; Gaussian, Inc.: Wallingford, CT, 2004.

as previously proposed³¹ using the broken atoms. The J values (defined in the isotropic Heisenberg spin Hamiltonian written in eq 2 and the inset of Figure 2) are given in the symmetry procedure to calculate the energy of the low spin states (Tables S3 and S4 in the Supporting Information).

$$H_{\text{iso}} = -2J_1(S_1S_2 + S_1'S_2') - 2J_2(S_1S_3 + S_1'S_3') - 2J_3(S_2S_3 + S_2'S_3') - 2J_4(S_1S_3' + S_3S_3' + S_3S_1') - 2J_5(S_3S_3') \quad (2)$$

The extracted coupling constants were all ferromagnetic (Table S5 in the Supporting Information), ranging from +0.6 to +80 cm^{-1} . It is to be noted that all of these values except J_1 are expected to be an overestimation of the true ones, as has been reported to be the case in such types of calculations involving EO azide-bridged Ni^{II} ions.³² In any case, this outcome suggests that $S_{\text{T}} = 6$ may be the spin ground state and, therefore, that the maximum of the $\chi_{\text{M}}T$ vs T plot could be caused by ZFS and/or intermolecular interactions.

The above information was used to fit the experimental curve in Figure 2 with the help of the program *MAGPACK*,³³ together with a least-squares fitting program,³⁴ using the spin Hamiltonian in eq 2, by imposing a positive (ferromagnetic) value to the coupling constants. Because the effects of ZFS and intercluster interactions are correlated, only either one or the other was considered in the fit. The fit including the second effect (as a zJ' parameter), incorporated in the calculation using the molecular-field approximation,³⁵ produced the following parameters (Figure 2, solid line); $J_1 = +0.05 \text{ cm}^{-1}$, $J_2 = +0.10 \text{ cm}^{-1}$, $J_3 = +18.8 \text{ cm}^{-1}$, $J_4 = +0.09 \text{ cm}^{-1}$, $J_5 = +5.65 \text{ cm}^{-1}$, $zJ' = -0.21 \text{ cm}^{-1}$, and $g = 2.26$. The procedure including instead single-ion ZFS (as a D parameter) yielded very similar results but a D value larger than that expected for Ni^{II} (our limit was established at 10 cm^{-1}), showing the influence of intermolecular interactions. Thus, the curve may be reproduced considering an $S = 6$ ground state if the effect of ZFS or intercluster interactions are considered. However, given their mutual influence, these cannot be discerned through this procedure and the results for zJ' or D have no real physical meaning.

Additional information was retrieved by analysis of isofield-reduced magnetization (M) measurements performed in the 1.8–7.8 K temperature range. The resulting M vs H/T plots (Figure 3) were fit by full diagonalization using the Hamiltonian in eq 3.

$$H = g\beta S_{\text{T}}B + D[S_{\text{Tz}}^2 - S(S+1)/3] + E(S_{\text{Tx}}^2 - S_{\text{Ty}}^2) \quad (3)$$

In this equation, D and E are the ground-state ZFS parameters for the whole cluster, and it is assumed that only

- (28) Becke, A. D. *J. Chem. Phys.* **1993**, *98*, 5648–5652.
 (29) Schafer, A.; Huber, C.; Ahlrichs, R. *J. Chem. Phys.* **1994**, *100*, 5829–5835.
 (30) Schafer, A.; Horn, H.; Ahlrichs, R. *J. Chem. Phys.* **1992**, *97*, 2571–2577.
 (31) Ruiz, E.; Rodriguez-Fortea, A.; Cano, J.; Alvarez, S.; Alemany, P. *J. Comput. Chem.* **2003**, *24*, 982–989.
 (32) Ruiz, E.; Cano, J.; Alvarez, S.; Alemany, P. *J. Am. Chem. Soc.* **1998**, *120*, 11122–11129.
 (33) Borrás-Almenar, J. J.; Clemente-Juan, J. M.; Coronado, E.; Tsukerblat, B. S. *J. Comput. Chem.* **2001**, *22*, 985–991.
 (34) Program 66. *Quantum Chemistry Program Exchange*; Indiana University: Bloomington, IN, 1965.
 (35) Kahn, O. *Molecular Magnetism*; VCH: New York, 1993; pp 131 and 132.

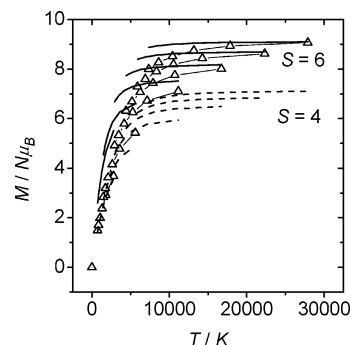


Figure 3. Isofield-reduced magnetization M vs H/T plots for complex **1** (fields: 0.5, 1, 2, 3, 4, and 5 T). Solid lines are fits for an isolated $S_{\text{T}} = 6$, and dashed lines are for $S_{\text{T}} = 4$ (see the text for details).

the ground state is populated. The other parameters have the usual meaning and also refer to the whole cluster. The best fit was found for $S_{\text{T}} = 6$, with $D = 2.76 \text{ cm}^{-1}$, $E = 0.27 \text{ cm}^{-1}$, and $g = 2.10$ (solid lines in Figure 3). The inaccuracies in this fit might be related to the fact that the ground state is not truly isolated or to the influence of intermolecular interactions. The fits for other ground states (see the dashed lines in Figure 3 for the fit with $S_{\text{T}} = 4$) were significantly worse than this fit, which favors the hypothesis that the ground state is $S_{\text{T}} = 6$. Nevertheless, the possibility of having an $S_{\text{T}} < 6$ ground state with very closely lying excited states such as $S_{\text{T}} = 6$ should not be disregarded. Measurements under an oscillating magnetic field reveal no signal for the out-of-phase component of the susceptibility, χ_{M}'' .

Ferromagnetic interactions for all of the pairings defined in complex **1** are not unexpected. These occur between Ni ions bridged by all EO N_3^- (J_4 and J_5)³⁶ or one EO N_3^- and one bridging phenoxide with acute Ni–O–Ni angles (see Figure S4 in the Supporting Information).³⁷ Coupling J_1 is expected to be close to zero because the bridges feature an acute Ni–O–Ni angle and a wider one.

In summary, the $[\text{Ni}_6]$ nuclearity in the form of four fused defective cubanes has been achieved as cluster **1** by the combined action of N_3^- bridges, together with the parent Schiff base ligand H_3L and its hydrolyzed form $\text{H}_2\text{L1}$. This introduces a set of μ - and μ_3 -mode azide and phenoxide bridging moieties that cause, within cluster **1**, dominant intramolecular ferromagnetic interactions. Bulk magnetization data, together with DFT calculations, suggest the presence of an $S_{\text{T}} = 6$ spin ground state.

Acknowledgment. D.M. acknowledges the CSIR, New Delhi, India, for her doctoral fellowship.

Supporting Information Available: Crystallographic data, tables of selected bond lengths and angles, CIFs, Schemes S1–S3, Figures S1–S9, Tables S1–S5, and syntheses and characterization of ligand H_3L and complex **1**. This material is available free of charge via the Internet at <http://pubs.acs.org>.

IC800188J

- (36) Ribas, J.; Escuer, A.; Monfort, M.; Vicente, R.; Cortés, R.; Lezama, L.; Rojo, T. *Coord. Chem. Rev.* **1999**, *195*, 1027–1068.
 (37) Clemente-Juan, J. M.; Chansou, B.; Donnadieu, B.; Tuchagues, J. P. *Inorg. Chem.* **2000**, *39*, 5515–5519.